Ceramic-to-Metal Joints Brazed with Palladium Alloys

Silicon nitride-to-nickel joints with shear strengths of 75 to 105 MPa at 200° and 500°C make heat engine applications a possibility

BY J. H. SELVERIAN AND S. KANG

ABSTRACT. Several alloys containing palladium were considered for use in brazing ceramics to metals for heat engine applications: 60Pd-40Ni, 30Au-34Pd-36Ni, 50Au-25Pd-25Ni, 70Au-8Pd-22Ni, 93Au-5Pd-2Ni, and 82Au-18Ni (all in wt-%). Palladium filler metals were selected because of their oxidation resistance, ductility and relatively high melting points. The reactions and microstructures were studied in experimental brazed joints between silicon nitride and nickel. The joints brazed with the low-palladium alloys, 70Au-8Pd-22Ni, 93Au-5Pd-2Ni, and 82Au-18Ni, had shear strengths of 75 to 105 MPa (11 to 15 ksi) from 20° to 500°C (68° to 932°F). The joints brazed with the high-palladium alloys, 60Pd-40Ni, 30Au-34Pd-36Ni, and 50Au-25Pd-25Ni, all had shear strengths near zero. The nature of the reactions and microstructure in the brazed joints will be discussed.

Introduction

Ceramic-to-metal braze joints will experience great thermal and stress cycling when used in heat engines. The materials' system must withstand this cycling and provide a reliable, creep-resistant and oxidation-resistant joint. The materials' system consists of the ceramic and structural alloy materials, the filler metal, intermediate or compliant layers, and a coating on the ceramic. Intermediate layers aid in accommodating the strains resulting from differential expansion between the metal and ceramic components of the joint. Coatings on the ceramic are necessary to promote wetting and adhesion between the filler metal and ceramic (Ref. 1). Palladium-containing filler metals were studied for ceramic-to-metal joints for use in heat engines with service temperatures exceeding 650°C (1202°F). Palladium was added to increase the melting point of common ceramic-to-metal braze alloys. Silicon nitride is being considered for the ceramic component due to its high-temperature strength and its thermal shock, oxidation, and creep resistance. In this study, attention was focused on the reactions between the braze alloy, the coating and the silicon nitride.

J. H. SELVERIAN and S. KANG are with GTE Laboratories, Inc., 40 Sylvan Rd., Waltham, Mass.

Procedure

The joint system contained a nickel substrate, a filler metal, and a silicon nitride ceramic. The silicon nitride contained 13 wt-% Y_2O_3 and 2 wt-% Al_2O_3 as sintering aids, and was coated with 3 μm of titanium, zirconium, or hafnium, which served to promote wetting between the braze alloy and silicon nitride. The surface of the silicon nitride substrates were polished, prior to surfacing, to a finish of 0.1 μm. Coatings were electron beam evaporated onto the silicon nitride in a 10^{-3} Pa (10^{-5} torr) vacuum at 300°C (572°F).

Five braze alloys containing palladium were studied: 60Pd-40Ni, 30Au-34Pd-36Ni, 50Au-25Pd-25Ni, 70Au-8Pd-22Ni and 93Au-5Pd-2Ni, along with 82Au-18Ni (all compositions are reported in wt-%) — Fig. 1. All of the braze alloys except the 93Au-5Pd-2Ni alloy fall in a relatively straight line on liquidus surface of the Au-Pd-Ni ternary diagram (Ref. 2). There is a discrepancy between the liquidus of the braze alloys reported in this study (Table 1) and those from Fig. 1. The liquidus data presented in Table 1 are thought to be more accurate, based on the discussion in Ref. 2.

KEY WORDS

Ceramic-to-Metal Brazing
Silicon Nitride Brazing
Shear Testing
Palladium Braze Alloys
Gold Braze Alloys
Nickel Braze Alloys
Ti Coatings
Zr Coatings
Outgassing
Heat Engines

The Young's modulus (E), ultimate tensile strength (σ_T) and yield strength (σ_Y) of the alloys were measured with 0.051-mm (0.002-in.) thick dog bone-shaped foil samples —Table 1. The acoustic wave technique was used to measure Young's modulus of some braze alloys that were available in bulk form. A strain gauge was used on the other samples to monitor the elongation to determine the Young's modulus. The gauge length of the samples was 4.44 cm long and 1.27 cm wide (1.75 X 0.5 in.). These tensile samples were 10 cm (4 in.) in length. The braze alloy foils were vacuum annealed for 5 h at 900°C (1652°F) prior to testing. The 82Au-18Ni braze alloy foil was vacuum annealed for 5 h at 800°C (1472°F) due to its lower melting point.

Wetting tests were performed by melting braze alloy foil on Ti-, Zr-, or Hf-coated silicon nitride substrates, in a 10^{-3} Pa vacuum. The wetting angle was recorded as a function of time.

A Hitachi RMU6-E magnetic sector mass spectrometer attached to a vacuum tube furnace was used to measure the amount and type of residual gases in the braze alloys and to monitor the reactions occurring between the braze alloys and the coated silicon nitride. The gases evolved from the sample were collected and emitted into the mass spectrometer for analysis. The collection volume of the gases was 1.6 L and extended beyond the hot zone of the furnace. Since the vacuum gauge was mounted outside of the furnace hot zone, the pressure measured was the gas pressure at

Table 1—Liquidus (T_L) and Brazing (T_B) Temperatures of the Braze Alloys, along with Selected Room-Temperature Mechanical Properties of the Braze Alloy Foils, and the Room-Temperature Coefficient of Thermal Expansion (CTE).

Trade Name of Braze Alloy[a]	Au	Pd (wt-%)	Ni	T_L (°C)	T_B (°C)	E (GPa)	G (GPa)	υ	σ_T (MPa)	σ_y (MPa)	CTE (× 10^{-6}/°C)
Palni[b]	—	60	40	1238	1290	152.3	—	—	585	448	—
Palniro 4[c]	30	34	36	1169	1220	140.0	51.3	0.365	625	576	15.5
Palniro 1[c]	50	25	25	1121	1170	114.4	41.3	0.383	721	712	15.5
Palniro 7[c]	70	8	22	1037	1090	114.0	41.1	0.388	644	572	17.5
Experimental[b]	93	5	2	1082	1180	91.3	—	—	187	115	—
Nioro[b]	82	—	18	950	1000	99.0	—	—	744	592	17.5

(a) GTE WESGO, Belmont, Calif.
(b) Tensile properties were measured from 0.002-in.-thick foil samples, a strain rate of 0.02 in./s, and the strain was measured with a strain gauge. Some of the foil samples failed prematurely by tearing.
(c) Young's Modulus, shear modulus, and Poisson's ratio were measured by the acoustic wave technique.

an unknown intermediate temperature and was used only for comparing the wetting tests of different samples.

The braze alloys were melted on a 99.9% Al_2O_3 substrate, to prevent reactions, to identify the residual gases in the braze alloys. A sample was degassed by heating to 400°C (752°F) for 10 min in a cooler part of the tube furnace, then transferred into the furnace hot zone with a magnetic push rod. The furnace was at the brazing temperature for the particular alloy under study. The same method was used to measure gases evolved during reactions between the alloy and the Ti- and Zr-coated silicon nitride.

Joints were brazed by ramping to the brazing temperature (50°C/122°F above the liquidus temperature) and holding for 5 min in a vacuum of 10^{-3} Pa. Samples brazed with Au-5Pd-2Ni were heated 100°C (212°F) above the liquidus because the liquidus was incorrectly identified as 1131°C (2068°F). The samples were furnace cooled, sectioned, polished and examined in a scanning electron microscope (SEM).

Joints between nickel and Ti-coated silicon nitride were brazed for shear testing. A schematic of the shear test samples is shown in Fig. 2. Five shear tests were conducted at room temperature and at 500°C, in argon, for each of the six braze alloys, for a total of 60 tests. Both the silicon nitride and nickel were 3 mm (0.12 in.) thick and the joint area (ignoring unbonded area) was 0.96 cm^2 (0.15 $in.^2$). The same experimental setup used for shear testing was also used to conduct stress-rupture tests at 500°C. A constant load was applied to the brazed joint in the shear testing fixture and the time to failure was recorded.

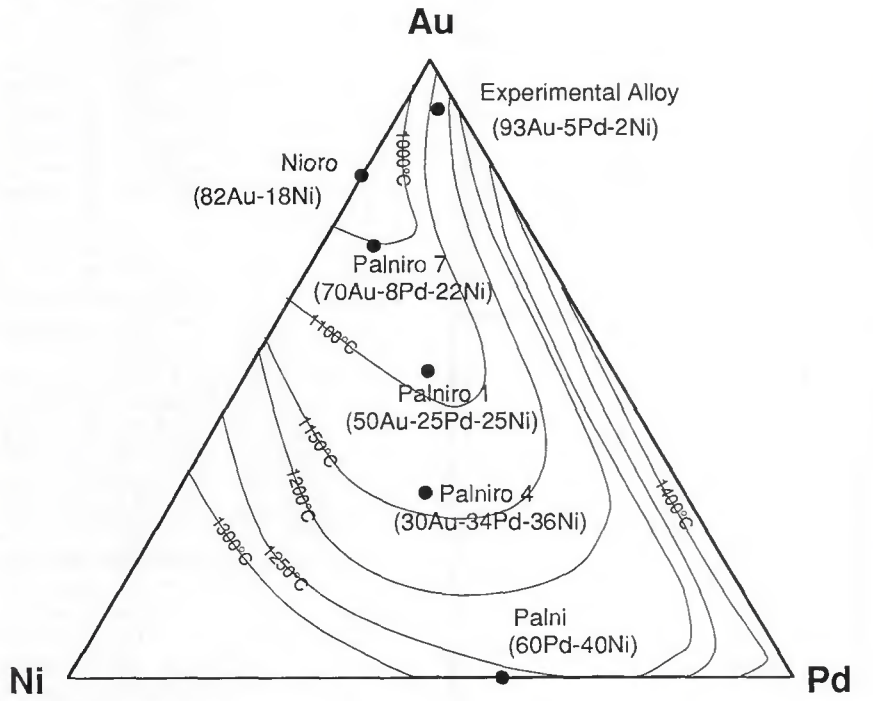

Fig. 1 — The composition of the braze alloys used plotted on the liquidus surface of the ternary Au-Pd-Ni phase diagram (wt-%). Liquidus surface is from Ref. 2.

Results and Discussion

Wetting Behavior and Outgassing

The results of the wetting tests on Ti-coated silicon nitride are shown in Fig. 3A. All six braze alloys wet the Ti-coated silicon nitride well, reaching a contact angle of approximately 10 deg after 2 min. In general, the reactions between the braze alloys and Ti-coated silicon nitride were moderate. The Ti coating was observed to react with silicon nitride to form TiN (Refs. 3–5).

Wetting tests were also performed on Hf- and Zr-coated silicon nitride substrates. All of the braze alloys wet Hf-coated silicon nitride except the 60Pd-40Ni braze alloy — Fig. 3B. During the wetting tests on Hf-coated silicon nitride, the Pd-containing braze alloys bubbled, indicating that gas was evolved. Severe gas evolution was also seen for the Pd-containing braze alloys on Zr-coated silicon nitride, and these wetting tests were not completed. Approximately 200 ppm of CO, CO_2 and H_2 were dissolved in each of the braze alloys, corresponding to 10^{-3} Pa of gas. The large amount of gas evolved during some of the wetting tests could not be explained by the comparatively small amount of residual gas present in the braze alloy foils.

A series of experiments designed to study the interaction between braze alloys and coated silicon nitride were conducted in a furnace/mass spectrometer unit. Table 2 shows the results of these investigations. Mass spectroscopy showed that most of the samples gave off hydrogen during the wetting tests. Part of this hydrogen came from the braze alloy itself. However, the majority of the hydrogen was released from the Ti and Zr coating when part of the coating was dissolved by the molten braze alloy. Titanium and zirconium are known to dissolve large amounts of hydrogen.

The 60Pd-40Ni braze alloy released a large amount of nitrogen during wetting tests on both Ti- and Zr-coated silicon nitride. More nitrogen gas was evolved when the braze alloys were melted on Zr-coated silicon nitride as compared to Ti-coated silicon nitride. The difference in behavior between Ti- and Zr-coated silicon nitride was unexpected since titanium and zirconium are both Group IVB elements and have many similar chemical characteristics.

While the amount of nitrogen evolution appeared to depend on the palladium content of the braze alloys (Fig. 4), the gas evolution was not caused by a direct reaction between palladium and silicon nitride. Palladium does not reduce silicon nitride to form a palladium silicide and nitrogen (Refs. 6, 7). The nitrogen evolution when the 60Pd-40Ni braze alloy wets Ti- or Zr-coated silicon nitride can be understood by the microstructure of the reaction zones.

Microstructure

Joints were made between nickel substrates and Ti-coated silicon nitride, using each of the braze alloys. They were then examined in an SEM. The brazed joints had similar microstructures. The width of the brazed region (Table 3) was determined from the width of the high-intensity region of a gold x-ray map. There was little reaction between the braze alloy and the Ti-coated silicon nitride except for the dissolution of part of the titanium coating. A 1-μm-thick Ti-rich layer remained at the silicon nitride surface with the remainder of the original 3-μm Ti-coating dissolving into the braze alloy. The major re-

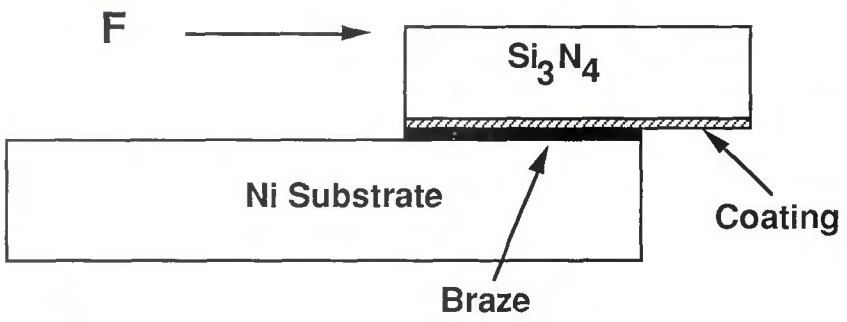

Fig. 2 — Schematic of brazed coupons used for shear testing.

Table 2—Mass Spectroscopy Results for Braze Alloy, Coating, Silicon Nitride Interactions in a 1.6 Liter Collection Volume

Sample	Gas Pressure Pa × 10^2 (× 10^6 Torr)	Test Temperature (°C)	P_{N_2} Pa × 10^2 (× 10^6 Torr)
Si_3N_4	2.5 (193)	1300	2.0 (154)
Ti-coated Si_3N_4	0.17 (13)[b]	1290	0.05 (4)
Zr-coated Si_3N_4	0.66 (50)	1290	0.33 (25)
(60Pd-40Ni)/Si_3N_4	3.2 (244)[b]	1290	2.1 (159)
(60Pd-40Ni)/(Ti-coated Si_3N_4)	2.2 (165)[c]	1290	1.8 (135)
(60Pd-40Ni)/(Zr-coated Si_3N_4)	7.3 (553)[b]	1290	6.6 (498)
(30 Au-34Pd-36Ni)/(Ti-coated Si_3N_4)	1.0 (76)[c]	1220	0.58 (44)
(30 Au-34Pd-36Ni)/(Zr-coated Si_3N_4)	6.6 (500)	1220	6.6 (500)
(50 Au-25Pd-25Ni)/(Ti-coated Si_3N_4)	1.1 (83)[c]	1190	0.36 (27)
(50 Au-25Pd-25Ni)/(Zr-coated Si_3N_4)	5.5 (415)	1190	5.5 (415)
(70 Au-8Pd-22Ni)/(Ti-coated Si_3N_4)	0.47 (36)[c]	1090	0.2 (15)
(70 Au-8Pd-22Ni)/(Zr-coated Si_3N_4)	1.5 (111)	1090	0.89 (67)
(93 Au-5Pd-2Ni)/Si_3N_4	2.1 (158)	1200	1.5 (110)
(93 Au-5Pd-2Ni)/(Ti-coated Si_3N_4)	0.74 (56)	1200	0.04 (3)
(93 Au-5Pd-2Ni)/(Zr-coated Si_3N_4)	1.7 (131)	1200	1.1 (79)
(82 Au-18Ni)/(Ti-coated Si_3N_4)	1.0 (78)	1000	0 (0)
(82 Au-18Ni)/(Ti-coated Si_3N_4)	0.53 (40)	1290	0.13 (10)
(82 Au-18Ni)/(Zr-coated Si_3N_4)	1.3 (98)	1000	0.4 (30)
(82 Au-18Ni)/(Zr-coated Si_3N_4)	4.4 (329)	1290	4.4 (329)

(a) P_{N_2} is the partial pressure due to nitrogen. The remaining pressure was mostly due to hydrogen.
(b) Normalized from a 3.5 liter to a 1.6 liter volume.
(c) Average of two trials.

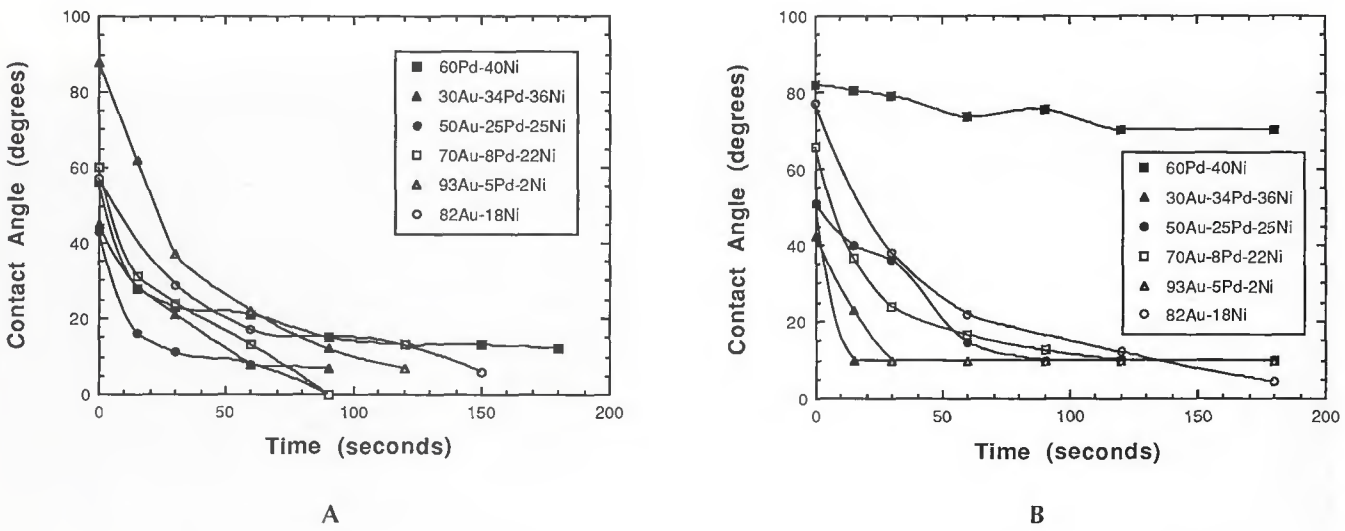

Fig. 3 — Wetting angle diagrams. A — Pd-containing braze alloys on Ti-coated silicon nitride; B — Pd-containing braze alloys on Hf-coated silicon nitride.

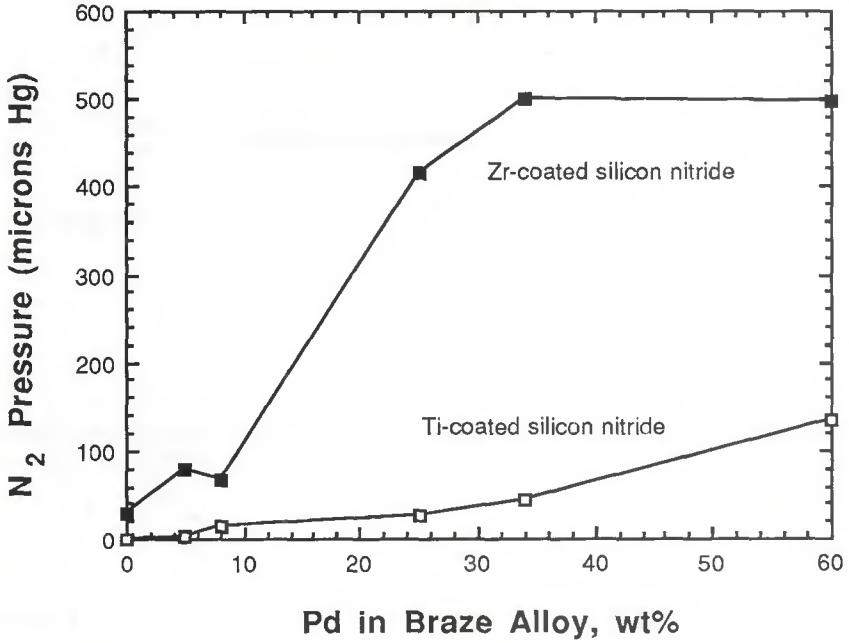

Fig. 4 — Plot of nitrogen partial pressure vs. palladium content of braze alloys for wetting of braze alloys on Ti- and Zr-coated silicon nitride.

Table 3—Width of Brazed Region Measured from the Gold X-Ray Map of Each Joint.

Braze Alloy (Wt-%)			Width of Brazed Region	T_B	T_B-T_L
Au	Pd	Ni	(μm)	(°C)	(°C)
—	60	40	>60	1290	52
30	34	36	20	1220	51
50	25	25	25	1170	49
70	8	22	40	1090	53
93	5	2	50	1180	98
82	—	18	20	1000	50

action involved dissolution of the base nickel by the molten braze alloys. The amount of dissolution of the nickel was related to a combined effect of high brazing temperature and the large solubility of nickel by the braze alloy.

SEM images of a joint brazed with the 70Au-8Pd-22Ni alloy are shown in Fig. 5. The gold and palladium were uniformly distributed in the brazed joint. The series of dark particles near the interface in Fig. 5A is a Ti-Ni phase.

Figure 5A shows signs of mechanical interlocking at the braze alloy/Si_3N_4 interface. However, mechanical interlocking was not widely evident in these brazed joints, and it is believed to have accounted for a small percentage of the shear strength.

Reactions between the Ti coating and Zr coating with the silicon nitride in joints brazed with the 50Au-25Pd-25Ni alloy were examined with an electron microprobe analyzer (EPMA) equipped with wavelength dispersive x-ray spectrometers. These joints were held at the brazing temperature (1170°C/2138°F) for 1 h to allow a wide reaction layer to form for easier analysis. Figures 6 and 7 show titanium, zirconium and nitrogen x-ray line traces across the coating/Si_3N_4 interface. These line traces are qualitative, and the ratio of the Ti and N signals is a complex function of the actual concentrations of these elements. There was an important difference in the behavior of the Ti coating and Zr coating on silicon nitride. The plateau regions in the nitrogen and titanium line scans (Fig. 6) indicate that titanium reacted with the silicon nitride to form a 2.5-μm-thick titanium nitride layer, possibly composed of two forms of titanium nitride. However, the lack of a plateau region in the nitrogen and zirconium line scans indicated that the reaction between zirconium and silicon nitride was a dissolution of nitrogen into the zirconium without compound formation — Fig. 7. The Zr-rich region was 1.8 μm wide in this joint.

The bulk braze alloy regions of both the Ti- and Zr-coated silicon nitride joints brazed with the 50Au-25Pd-25Ni alloy consisted of ternary Au-Pd-Ni phases. Little silicon was seen in the braze alloy of the Ti-coated silicon nitride joint. However, the joint with the Zr-coated silicon nitride had an additional phase present, a ternary silicide with an approximate composition of 39Ni-37Pd-24Si, determined by EMPA. The larger nitrogen partial pressure and the significant amount of silicon in the

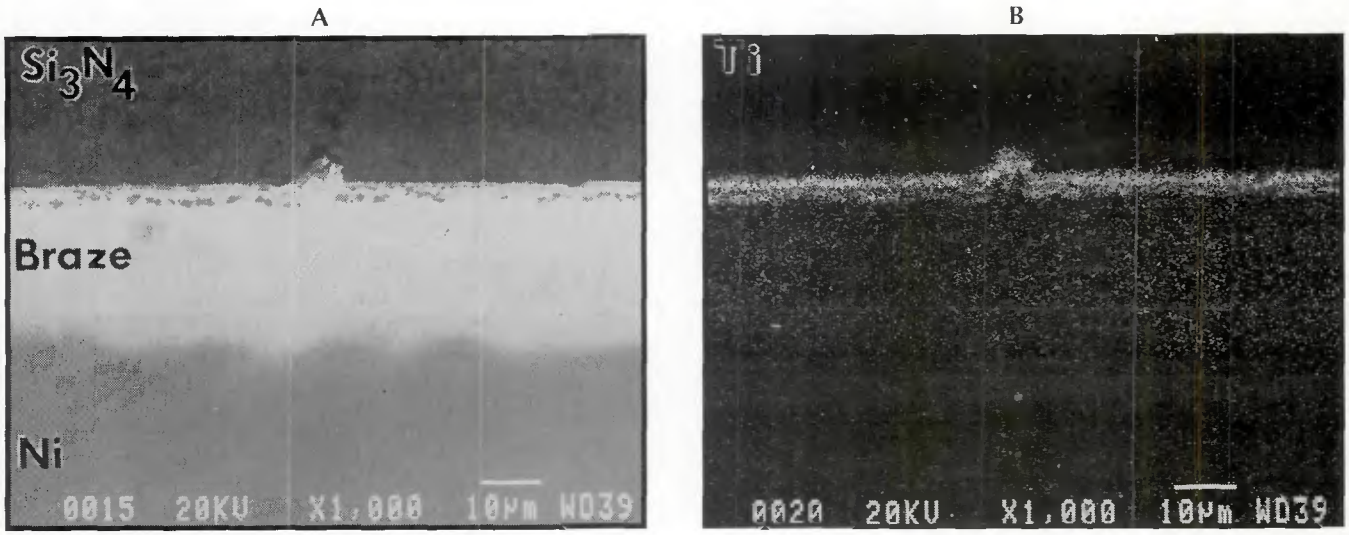

Fig. 5 — SEM images of brazed joint between nickel substrates and Ti-coated silicon nitride with the 70Au-8Pd-22Ni braze alloy. A — Backscattered electron image; B — titanium x-ray map.

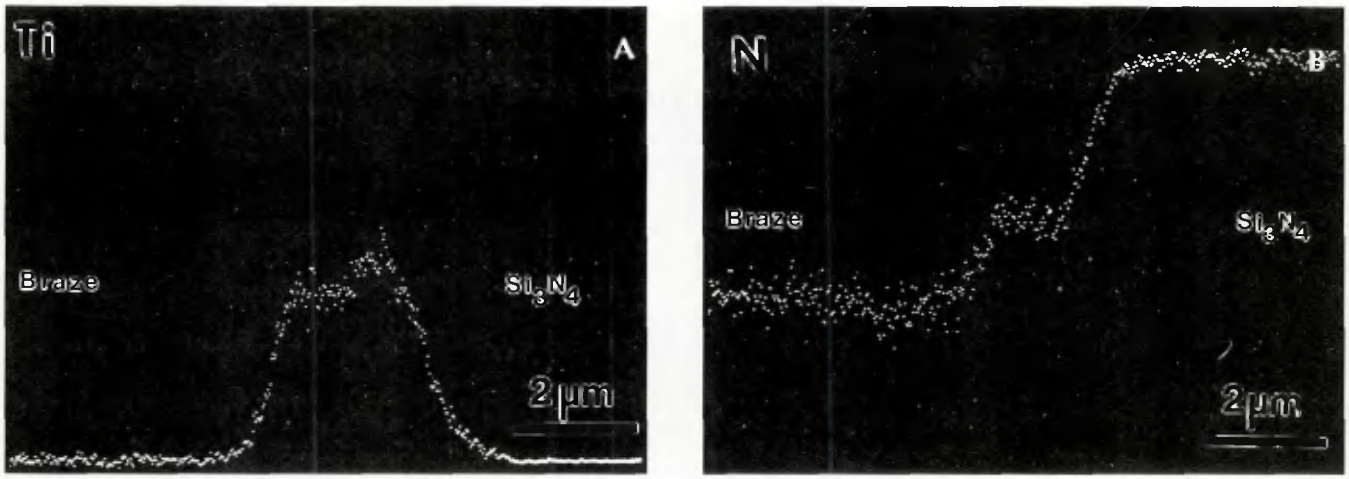

Fig. 6 — X-ray line scans across the Ti-coating/Si_3N_4 interface in a joint between Ti-coated silicon nitride and nickel brazed with 50Au-25Pd-25Ni alloy for 1 h. A — Titanium x-ray line scan; B — nitrogen x-ray line scan. The scan was 11.5 μm long.

braze alloy layer of the Zr-coated silicon nitride joints implied that the reaction rate of the Zr-coated silicon nitride systems was faster than that of the Ti-coated silicon nitride systems.

The difference in outgassing behavior between the Ti- and Zr-coated silicon nitride can be explained by the microstructures described above. When titanium reacted with silicon nitride, one or two layers of a titanium nitride were formed. The titanium nitride layer prevented further reaction between the titanium and braze alloy with the silicon nitride. However, when zirconium reacted with silicon nitride, no zirconium nitride layer was formed (Ref. 8). We hypothesize that the reaction between the braze alloy and the Zr-coated silicon nitride proceeded as follows: the silicon nitride decomposed, silicon diffused through the zirconium layer and reacted with the braze alloy forming the ternary silicide, some nitrogen dissolved in the zirconium, and the remainder of the nitrogen bubbled off into the vacuum.

Different braze alloys on the same substrate resulted in different amounts of nitrogen evolution. This was primarily attributed to different reaction temperatures since the high-palladium braze alloys have higher melting points. Figure 8 shows the nitrogen partial pressure replotted as a function of temperature. There was a strong correspondence between temperature and P_{N_2}. The last four wetting tests listed in Table 2 clarify the effect of temperature on nitrogen evolution. The 82Au-18Ni alloy on Zr-coated silicon nitride released 4 X 10^{-3} Pa (3 X 10^{-5} torr) of nitrogen at 1000°C (1832°F) and released 4.4 X 10^{-2} Pa (3.29 X 10^{-4} torr) of nitrogen at 1290°C (2354°F). This indicates the significance of temperature on the nitrogen gas evolution. The effect of temperature on the nitrogen evolution from Ti-coated silicon nitride was minor, as shown by the results of the same type of experiments run on Ti-coated silicon nitride — Table 2. The effect of palladium appeared to be of slightly less significance, although important, in the amount of nitrogen evolved. This was shown by comparing wetting tests carried out at 1290°C on Zr-coated silicon nitride with the 82Au-18Ni (4.4 X 10^{-2} Pa N_2) and the 60Pd-40Ni (6.6 X 10^{-2} Pa N_2) braze alloys.

The behavior of the 93Au-5Pd-2Ni and 50Au-25Pd-25Ni braze alloys on Zr-coated silicon nitride indicates the synergistic effect of temperature and palladium content on nitrogen evolution — Table 1 and Fig. 8. The 93Au-5Pd-2Ni and 50Au-25Pd-25Ni braze alloys were held at essentially the same temperatures but evolved 1.7 X 10^{-2} and 5.5 X 10^{-2} Pa (1.31 X 10^{-4} and 4.15 X 10^{-4} torr) of nitrogen, respectively. The effect of the interaction between temperature and palladium content on nitrogen evolution was not clear and requires further study.

The strong temperature dependence and the difference in reaction zones be-

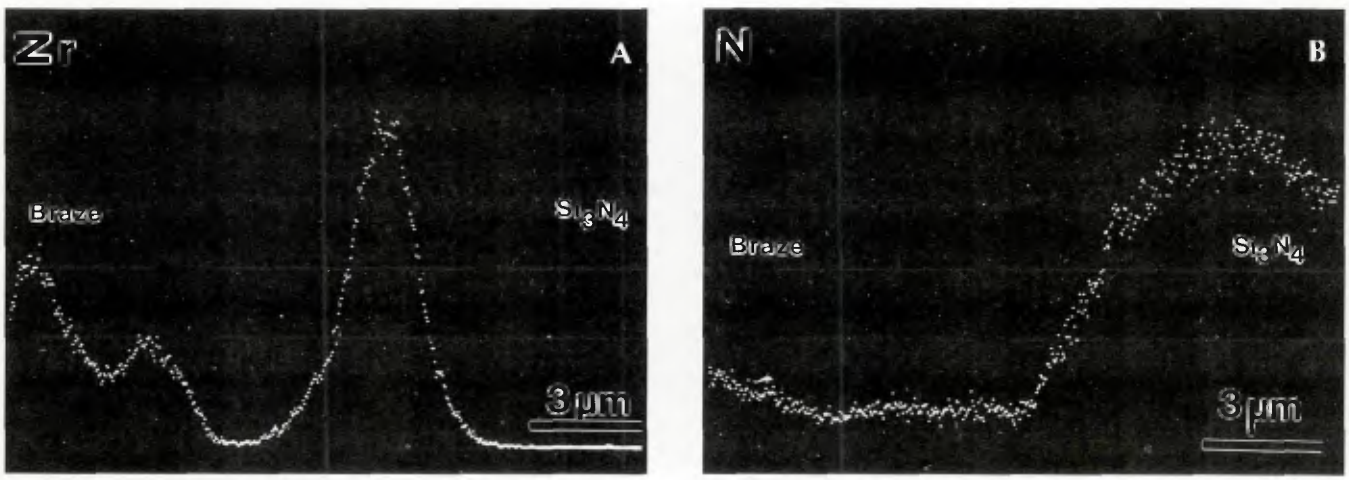

Fig. 7 — X-ray line scans across the Zr-coating/Si_3N_4 interface in a joint between Zr-coated silicon nitride and nickel brazed with the 50Au-25Pd-25Ni alloy for 1 h. A — Zirconium x-ray line scan; B — nitrogen x-ray line scan. The scan was 19 μm long.

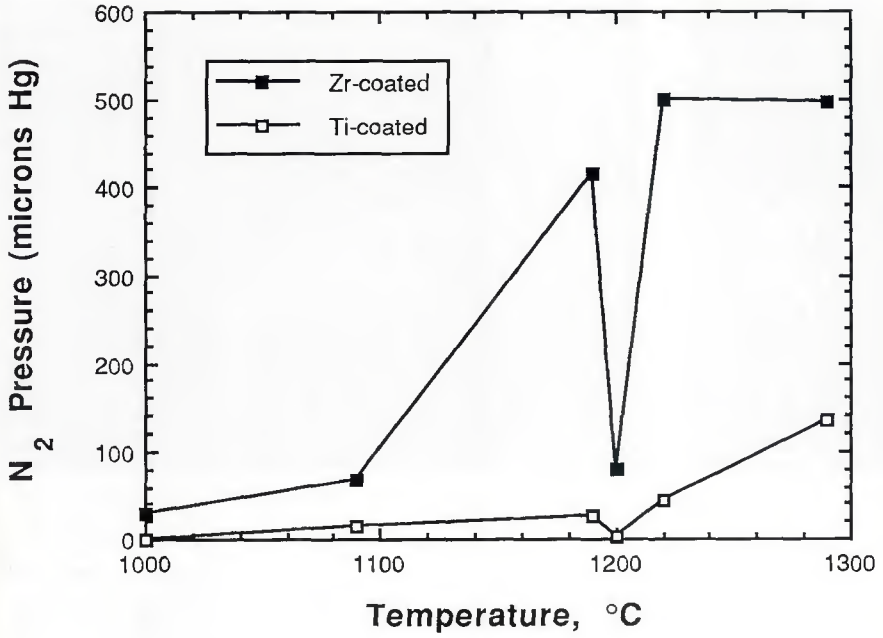

Fig. 8 — Plot of nitrogen partial pressure vs. reaction temperature of braze alloys for wetting of braze alloys on Ti- and Zr-coated nitride.

tween the Ti- and Zr-coated silicon nitride substrates suggested that the diffusion of nitrogen through the TiN or zirconium layer controlled the reaction rate and, therefore, the nitrogen evolution. The diffusion coefficient of nitrogen in zirconium at 1290°C is 8.1 X 10^{-7} cm^2/s with an activation energy of 140 kJ/mole (Ref. 9). Therefore, the reaction between zirconium and silicon nitride at 1290°C should evolve approximately ten times more nitrogen than the same reaction would at 1000°C, as supported by Table 2. The diffusion coefficient of nitrogen in TiN is not known. However, as an approximation, the diffusivity of carbon in TiC was reported as 10^{-11} to 10^{-9} cm^2/s with an activation of 330 kJ/mole (Ref. 10). We hypothesize that the difference in behavior between Ti- and Zr-coated silicon nitride was due to the nature of the diffusion process. The TiN layer that formed in the Ti-coated silicon nitride samples acted as a diffusion barrier and inhibited the reactions between the titanium and the silicon nitride. However, in the Zr-coated silicon nitride samples, the zirconium layer allowed for comparatively rapid diffusion and a faster reaction rate between zirconium and silicon nitride.

Mechanical Testing

Braze Alloy Foils. The tensile properties of the annealed braze alloy foils are listed in Table 1. A range of Young's moduli and yield strengths are represented by these braze alloys.

Shear Tests. The results of the room-temperature and 500°C shear tests are summarized in Tables 4 and 5. In most of the 500°C tests, the nickel substrate was slightly bent during shear testing, which may have influenced the measured strength values. All of the silicon nitride pieces were Ti-coated. Brazed joints with Zr- and Hf-coated silicon nitride were not tested due to the bubbling problem discussed earlier.

The joints brazed with the low-palladium alloys (70Au-8Pd-22Ni, 93Au-5Pd-2Ni, and 82Au-18Ni) had the highest shear strengths. The average shear strengths at room temperature were 99, 77 and 82 MPa (14, 11, 12 ksi), respectively, and were 105, 85 and 104 MPa (15, 12, 15 ksi) at 500°C, respectively. The differences between the room-temperature and 500°C shear strengths of the brazed joints were not statistically significant. However, the shear strengths were expected to be higher at 500°C than at room temperature due to a reduction in residual stress in the silicon nitride near the interface. The residual stress in this type of brazed joint with the 82Au-18Ni braze is approximately 150 to 200 MPa (22 to 29 ksi) at room temperature (Ref. 11). The larger residual stress at room temperature may explain the larger standard deviation of the joints tested at room temperature as compared to the joints tested at 500°C. If more shear tests were conducted, it is felt that the expected difference between the room-temperature and 500°C joint strengths would become statistically apparent. The joints brazed with the 70Au-8Pd-22Ni alloy may be slightly stronger than those brazed with the 93Au-5Pd-2Ni alloy at 500°C. More testing is required before a definite statement can be made.

The Weibull modulus of silicon nitride ceramic used in this study was measured by four-point bend tests as 12. The data from the room-temperature and 500°C shear tests of the joints brazed with the 70Au-8Pd-22Ni, 93Au-5Pd-2Ni, and 82Au-18Ni braze alloys were combined to calculate a Weibull modulus for these brazed joints — Fig. 9. The Weibull modulus was calculated to be approximately 4. The different tests were combined since there was not a significant difference between the different joints and test conditions. This composite Weibull modulus is not an exact value, since it came from different types of samples; however, it is a useful approximation. The brazing process

Table 4—Results from Room-Temperature and 500°C Shear Tests between Nickel Substrates and Ti-Coated Silicon Nitride.

Braze Alloy Au Pd Ni Wt-%			Failure Load (kN) 25°C Sample No.								500°C) Sample No.							
			1	2	3	4	5	6	7	Ave.	1	2	3	4	5	6	7	Ave.
—	60	40	1.6	*	*	*	*	—	—	1.6	2.6	4.4	3.2	0.8	*	—	—	2.8
30	34	36	0.2	0.5	*	*	*	—	—	0.4	3.3	*	*	*	*	—	—	3.3
50	25	25	*	*	*	*	*	—	—	*	*	*	*	*	*	—	—	*
70	8	22	9.9	7.1	6.4	7.6	18.5	6.8	9.3	10.0	10.5	11.6	9.2	9.9	11.7	7.6	9.4	10.6
93	5	2	6.9	4.2	10.4	8.2	7.7	—	—	8.4	4.7	7.3	9.5	10.0	8.7	—	—	8.0
82	—	18	5.5	2.5	7.4	10.2	2.4	12.8	13.7	7.8	7.9	10.9	7.3	10.0	8.6	12.3	11.9	8.9

* Indicates that the sample broke during handling and could not be tested.
— Indicates that no sample was brazed.

caused a substantial drop in the Weibull modulus of the silicon nitride in the brazed joint. This decrease in Weibull modulus was probably related to the residual stress induced in the joint by the coefficient of thermal expansion (CTE) mismatch of the joint materials and to the reaction between the Ti coating and silicon nitride. A recent study on brazing silicon nitride to metal with reactive braze alloys reported a similar drop in the Weibull modulus from 15 to 3 (Ref. 12).

A difference in the shear strengths of the joints brazed with the 70Au-8Pd-22Ni, 93Au-5Pd-2Ni, and 82Au-18Ni alloys was expected. The 93Au-5Pd-2Ni braze alloy had a significantly lower yield stress than either the 70Au-8Pd-22Ni or 82Au-18Ni alloys and was expected to yield upon cooling from the brazing temperature to relieve the most severe residual stresses. The lack of difference in shear strengths between the joints brazed with the 70Au-8Pd-22Ni, 93Au-5Pd-2Ni, and 82Au-18Ni alloys may be attributed to problems in processing and testing the ceramic-metal joints.

Joints brazed with the high-palladium alloys (60Pd-40Ni, 50Au-25Pd-25Ni, and 30Au-34Pd-36Ni) had very low shear strength values. All were below 35 MPa (5 ksi). Most of the coupons brazed with the high-palladium alloys broke during handling. Only 12 samples out of 30 survived handling and were tested. All of the samples brazed with the 50Au-25Pd-25Ni alloy cracked in the silicon nitride during cooling and were not tested. A schematic of the type of cracks seen in the silicon nitride is shown in Fig. 10. The cracks often propagated all the way through the silicon nitride.

The joints that cracked on cooling from the brazing temperature were made with either a high-yield-strength braze alloy or with a high-temperature braze alloy. These types of braze alloys subjected the ceramic to large thermal stresses. Braze alloys with high yield strengths and high Young's moduli transfer the stresses due to CTE mismatch to the ceramic more effectively than do braze alloys with low yield strengths and low Young's moduli.

There was not a significant difference in the fracture mode of any of the joints except for those brazed with the 60Pd-40Ni alloy and tested at 500°C. Most of the joints fractured in the ceramic (at a depth of approximately 1- to 2-mm/0.04 to 0.08 in.) with the crack propagating parallel to the interface. Fracture in the ceramic was expected due to the increase of thermal mismatch stresses, which reduce the ceramic's fracture strength (Refs. 11, 13). Fracture surfaces from joints brazed with the 60Pd-40Ni and 50Au-25Pd-25Ni alloys are shown in Fig. 11. The fracture surface of the 50Au-25Pd-25Ni joint was typical of the fracture surfaces from the four other braze alloys. The joints brazed with the 60Pd-40Ni alloy had approximately 30% unbonded area, compared to ~5% unbonded area for joints brazed with the other alloys. This large amount of unbonded area in the 60Pd-40Ni joints was attributed to nitrogen gas evolution, as seen during the wetting tests. The nitrogen bubbled through the molten braze alloy and caused large amounts of unbonded area, which favored interfacial failure.

Table 5—Shear Strengths from Room-Temperature and 500°C Shear Tests in Table 4

Braze Alloy (Wt-%)			Failure Shear Stress, MPa (ksi)			
			25°C		500°C	
Au	Pd	Ni	Mean[a]	Std. Dev.[a]	Mean[a]	Std. Dev.[a]
—	60	40	17.1 (2.5)[b]	—	28.8 (4.2)	15.9
30	34	36	3.7 (0.5)	2.3	35.7 (5.2)[b]	—
50	25	25	—	—	—	—
70	8	22	98.7 (14.3)	44.5	105.2 (15.3)	15.3
93	5	2	76.8 (11.1)	23.8	85.0 (12.3)	22.5
82	—	18	81.6 (11.8)	48.5	103.8 (15.1)	20.3

[a]Samples that broke during handling were not included in these figures.
[b]No standard deviation is reported because only one sample was successfully tested.

The results of preliminary stress-rupture testing of the brazed joints are shown in Fig. 12. Only two of the braze alloys have been tested to date. The joints brazed with the 82Au-18Ni and the 70Au-8Pd-22Ni alloys resulted in essentially identical stress-rupture behavior.

Summary

Six braze alloys in the Au-Pd-Ni system were studied for brazing silicon nitride to nickel. The reactions, microstructure, and shear strengths of the brazed joints were examined. Palladium was added to increase the melting point

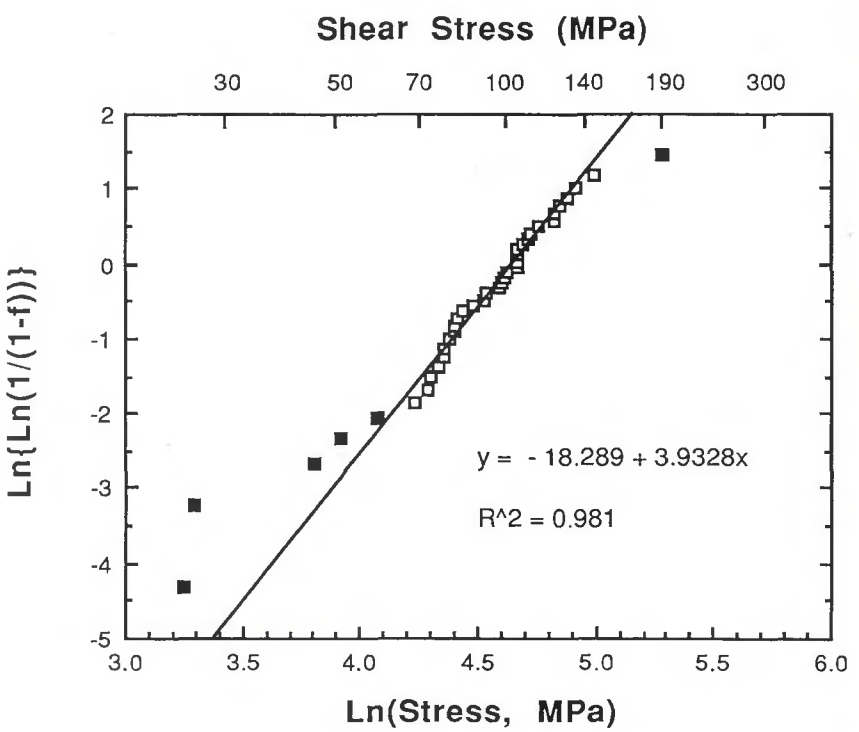

Fig. 9 — Weibull plot of the room-temperature and 500°C shear strengths from the 70Au-8Pd-22Ni, 93Au-5Pd-2Ni and 82Au-18Ni braze alloys. The solid-black data points were not included in the calculation of the Weibull modulus.

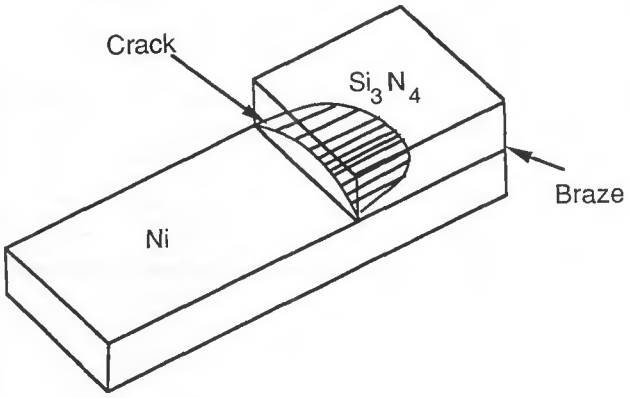

Fig. 10 — Crack in shear test samples that forms on cooling. The crack shown here did not propagate all the way through the silicon nitride. However, the samples with this type of crack broke during handling and could not be tested.

Fig. 11 — Fracture surfaces from shear tested joints brazed with 30Au-34Pd-36Ni (top) and 60 Pd-40Ni.

of Au-based braze alloys for high-temperature applications. The wetting behavior of these alloys and Ti-, Zr- and Hf-coated silicon nitride was also studied. All of the braze alloys wet the Ti-coated silicon nitride well. However, problems were encountered with the high-palladium alloys (60Pd-40Ni, 50Au-25Pd-25Ni and 30Au-34Pd-36Ni) on the Zr and Hf coatings. Bubbling of the molten braze alloy was observed. This bubbling was attributed to the different reactions between the Ti coating and Zr coating with the silicon nitride. Titanium reacts with silicon nitride to form a titanium nitride layer. Zirconium does not form a zirconium nitride layer but instead takes nitrogen into solid solution, releasing the nitrogen, and is more reactive with the silicon nitride.

Joints brazed with the high-palladium alloys also had the lowest room-temperature and 500°C shear strengths and consistently resulted in poor joint quality. Joints brazed with the low-palladium alloys had good shear strengths at room temperature and 500°C: 75 to 100 MPa (11 to 14 ksi) and 85 to 105 MPa (12 to 15 ksi), respectively. The brazing process damaged the silicon nitride to a large extent, and the Weibull modulus of the silicon nitride decreased from 12 to 4.

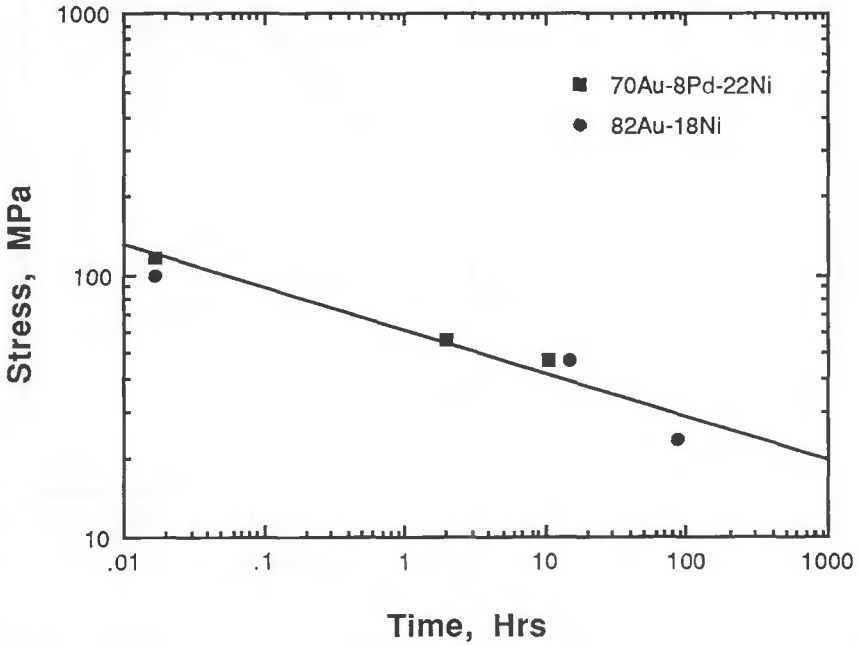

Fig. 12 — Results from 500°C stress rupture tests of joints brazed with the 70Au-8Pd-22Ni and 82Au-18Ni braze alloys.

Acknowledgments

This research was sponsored, in part, by the U.S. Department of Energy, Assistant Secretary for Conservation and Renewable Energy, Office of Transportation Systems, as part of the Ceramic Technology for Advanced Heat Engines Project of the Advanced Materials Development Program, under contract DE-AC05-840R21400 with Martin Marietta Energy Systems, Inc.

The participation in the experimental program by Dan Bazinet and Glenn McCloud is gratefully acknowledged. Assistance from the Materials Characterization Department, particularly from Dan Oblas, George Werber, Jody Harris and Jesse Hefter, was much appreciated.

References

1. Santella, M. 1988. Brazing of titanium-vapor-coated silicon nitride. *Advanced Ceramic Materials* 3 (5):457–462.

2. Prince, A., Raynor, G. V., and Evans, D. S. 1990. Phase diagrams of ternary gold alloys. p. 322. London, England, The Institute of Metals.

3. Kang, S., Dunn, E. M., Selverian, J. H., and Kim, H. J. 1989. Issues in ceramic-to-metal joining: an investigation of brazing a silicon nitride-based ceramic to a low-expansion superalloy. *American Ceramic Society Bulletin* 68(9):1608–1617.

4. Barbour, J. C., Kuiper, A. E. T., Willemsen, M. F. C., and Reader, A. H. 1987. Thin-film reaction between Ti and Si_3N_4. *Applied Physics Letters* 50(15):953–955.

5. Morgan, A. E., Broadbent, E. K., and Sadana, D. K. 1986. Reaction of titanium with silicon nitride under rapid thermal annealing. *Applied Physics Letters* 49 (19):1236–1238.

6. Chart, T. G. 1973. Thermochemical data for transition metal-silicon systems. *High Temperatures - High Pressures* 5:241–252.

7. Kubaschewski, O., and Alcock, C. B. 1979. *Metallurgical Thermochemistry.* p.

310. New York, N.Y., Pergamon Press.

8. Tomsia, A. P., and Loehman, R. E. 1990. Reaction mechanisms in active metal brazing. Proc. of the 92nd Amer. Ceram. Soc. Annual Meeting, Abstract 246.

9. Mangio, C. A. 1955. Diffusion: the metallurgy of zirconium. B. Lustman and F. Kerze, Jr., eds., p. 422, New York, N.Y., McGraw-Hill.

10. van Loo. F. J. J., and Bastin, G. F. 1989. On the diffusion of carbon in titanium carbide. *Metallurgical Transactions* A 20A(3):403–411.

11. Kang, S., Selverian, J. H., Kim, H., O'Neil, D., and Kim, K. 1990. Analytical and experimental evaluation of joining silicon nitride to metal and silicon carbide to metal for advanced heat engine applications. Department of Energy Contract No. DE-AC05-840R21400.

12. Lugscheider, E., and Tillman, W. 1990. Development of new active filler metals in a Ag-Cu-Hf system. *Welding Journal* 69(11):416-s to 421-s.

13. Evans, A. G., Dalgleish, B. J., He, M., and Hutchinson, I. W. 1989. On crack path selection and the interface fracture energy in bimaterial systems. *Acta Metallurgica* 37(12):3249–3254.

WRC Bulletin 360
January 1991

Stress Indexes, Pressure Design and Stress Intensification Factors for Laterals in Piping

By E. C. Rodabaugh

The study described in this report was initiated in 1987 by the PVRC Design Division Committee on Piping, Pumps and Valves under a PVRC grant to E. C. Rodabaugh following an informal request from the ASME Boiler and Pressure Vessel Committee, Working Group on Piping (WGPD) (SGD) (SC-II) to develop stress indexes and stress intensification factors (*i*-factors) for piping system laterals that could be considered by the ASME Committee for incorporation into the code.

In this study, the author has considers all existing information on lateral connections in concert with existing design guidance for 90-deg branch connections; and has developed compatible design guidance for lateral connections for piping system design. As a corollary bonus, he has also extended the parameter range for the "B" stress indexes for 90-deg branch connections from d/D = 0.5 (the present code limit) to d/D = 1.0. Therefore, this report should be of significant interest to the B31 industrial piping code committees, as well as the ASME Boiler and Pressure Vessel Committee.

Publication of this bulletin was sponsored by the Committee on Piping, Pumps and Valves of the Design Division of the Pressure Vessel Research Council. The price of WRC Bulletin 360 is $30.00 per copy, plus $5.00 for U.S. and $10.00 for overseas, postage and handling. Orders should be sent with payment to the Welding Research Council, Room 1301, 345 E. 47th St., New York, NY 10017.

WRC Bulletin 363
May 1991

Recommended Practices in Elevated-Temperature Design: A Compendium of Breeder Reactor Experiences (1970–1987), Volume II—Preliminary Design and Simplified Methods

Edited by A. K. Dhalla

The recommended practices for elevated-temperature design of liquid metal fast breeder reactors (LMFBR) have been consolidated into four volumes to be published in four individual WRC bulletins.

Volume I: Current Status and Future Directions (WRC Bulletin 362)
Volume II: Preliminary Design and Simplified Methods (WRC Bulletin (363)
Volume III: Inelastic Analysis (WRC Bulletin 365)
Volume IV: Special Topics (WRC Bulletin 366)

In Volume II, preliminary design procedures are described that provided practical design and analysis guidelines for specific structural design problems encountered in the past. Also included is a detailed discussion of simplified methods to support both preliminary and final design evaluations.

Publication of this bulletin was sponsored by the Committee on Elevated Temperature Design of the Pressure Vessel Research Council. The price of WRC Bulletin 363 is $40.00 per copy, plus $5.00 for U.S. and $10.00 for overseas, postage and handling. Orders should be sent with payment to the Welding Research Council, Room 1301, 345 E. 47th St., New York, NY 10017.

First Announcement and Call for Papers

1992 NORTH AMERICAN WELDING RESEARCH CONFERENCE

RECENT DEVELOPMENTS IN THE JOINING OF STAINLESS STEELS AND HIGH ALLOYS

Columbus, Ohio, October 19-21, 1992
Hyatt on Capitol Square

The Eighth Annual North American Conference on Welding Research will provide a state-of-the-art review of recent developments and advances in the joining technology for stainless steels, including austenitic and "super" austenitic, duplex and "super" duplex, ferritic, martensitic and specialty grades, and high alloy Ni-base and Co-base alloys used in corrosive and/or high temperature applications.

Papers are sought in the following areas:

- **Welding metallurgy**
- **Welding process development (arc and HED processes)**
- **Welding process development (solid state processes)**
- **Weld properties**
- **Design and Fitness-for-Service**
- **Corrosion behavior**
- **Total Quality Joining**

For more information on the technical content of the conference, contact:

Dr. John Lippold
Manager, Research Development
EWI
1100 Kinnear Road
Columbus, Ohio, USA 43212
Phone (614) 486-9400, FAX (614)486-9528